Exacting Predictions by Cybernetic Model Confirmed Experimentally: Steady State Multiplicity in the Chemostat

Jin Il Kim and Hyun-Seob Song
School of Chemical Engineering, Purdue University, West Lafayette, IN 47907

Sunil R. Sunkara and Arvind Lali
DBT-ICT-Centre for Energy Biosciences, Institute of Chemical Technology, Nathalal Parikh Marg, Matunga, Mumbai 400 019, India

Doraiswami Ramkrishna
School of Chemical Engineering, Purdue University, West Lafayette, IN 47907

DOI 10.1002/btpr.1583
Published online in Wiley Online Library (wileyonlinelibrary.com).

We demonstrate strong experimental support for the cybernetic model based on maximizing carbon uptake rate in describing the microorganism's regulatory behavior by verifying exacting predictions of steady state multiplicity in a chemostat. Experiments with a feed mixture of glucose and pyruvate show multiple steady state behavior as predicted by the cybernetic model. When multiplicity occurs at a dilution (growth) rate, it results in hysteretic behavior following switches in dilution rate from above and below. This phenomenon is caused by transient paths leading to different steady states through dynamic maximization of the carbon uptake rate. Thus steady state multiplicity is a manifestation of the nonlinearity arising from cybernetic mechanisms rather than of the nonlinear kinetics. The predicted metabolic multiplicity would extend to intracellular states such as enzyme levels and fluxes to be verified in future experiments. © 2012 American Institute of Chemical Engineers *Biotechnol. Prog.,* 000: 000–000, 2012
Keywords: cybernetic mechanism, multiplicity, chemostat, Escherichia coli*, metabolic regulation*

Introduction

Microbes significantly impact humans as many useful products result from their metabolism. The important field of metabolic engineering seeks to make genetic changes in an organism towards maximizing the productivity of desired products of very high impact such as biofuels, drugs, and numerous others. Consequently, the cultivation, control and design of microorganisms are an important aspect of modern biotechnology. Metabolic processes are, however, subject to strict genetic control of the cell's protein synthesis machinery resulting in preferential responses by the organism to its environment and varying distribution of metabolic products. This control is understood to be accomplished through genetic switches triggered by various signals. A strictly cause-and-effect based scientific approach to describing such control is untenable because of the complexity of what is known and the immensity of what is unknown. Recently, Kim et al. (2008)[1] have shown how the hybrid cybernetic model (HCM) describes different uptake patterns of substrate mixtures of glucose and pyruvate by *Escherichia coli*. Their model is based on the cybernetic goal of maximizing carbon uptake rate.

In this article, we subject the cybernetic model of Kim et al. (2008),[1] maximizing carbon uptake rate, to more rigorous tests by comparing its predictions in a chemostat. Nonlinear analysis of the cybernetic model reveals many interesting results. Thus, for substrate feeds containing a mixture of glucose and pyruvate of appropriate composition, the model predicts multiple steady states. Calculations show that steady state multiplicity can be as high as 5 with 3 stable and 2 unstable. We desist from an exhaustive bifurcation analysis in this exercise as our goal has been identification of challenging and unusual scenarios for experimental verification. Steady state multiplicity has been reported in the literature[2] by models with kinetic mechanisms for metabolic regulation. This is a manifestation of kinetic nonlinearity. The multiplicity reported in this article is a consequence of the nonlinearity present in the cybernetic mechanism rather than of only the kinetic nonlinearity.

Our presentation begins by recapitulating the model by Kim et al. (2008)[1] followed by the results of computations on steady state concentrations of various fermentation products, residual substrate levels, and biomass. The extent to which the data conform to prediction is evaluated in detail in the Results and Discussion with Concluding Remarks reflecting on long term implications of this work.

Additional Supporting Information may be found in the online version of this article.

Current address of Jin Il Kim: Samsung Engineering Co., Ltd., 467-14 Samsung SEI Tower, Dogok 2 Dong, Gangnam-Gu, Seoul 135-856, Republic of Korea

Correspondence concerning this article should be addressed to D. Ramkrishna at this current address: Forney Hall of Chemical Engineering, 480 Stadium Mall Drive, West Lafayette, IN 47907-2100; ramkrish@ecn.purdue.edu.

Metabolic Model

Modeling framework

Dynamic metabolic behavior of microorganisms is suitably modeled using the hybrid cybernetic approach.[1,3] The "cybernetic" modeling approach describes cellular metabolism from the viewpoint that a microorganism is an optimal strategist making frugal use of limited internal resources to maximize its survival.[4,5] Metabolic regulation of enzyme synthesis and their activities is made as the outcome of such optimal allocation of resources. The HCM incorporates the concept of elementary modes (EMs)[6] into the cybernetic framework. EM is a metabolic pathway (or subnetwork) composed of a minimal set of reactions supporting a steady state operation of metabolism. Any feasible metabolic state can be represented by nonnegative combinations of EMs. HCM views EMs as cell's metabolic options, which are optimally modulated under dynamic environmental conditions such that a prescribed metabolic objective (such as the total carbon uptake flux) is maximized. An HCM for a chemostat can be given as follows:

$$\frac{d\mathbf{x}}{dt} = \mathbf{S_x Z r_M} c + D(\mathbf{x_{IN}} - \mathbf{x}) \tag{1}$$

where c is the biomass concentration, $\mathbf{x}$ is the vector of n_x concentrations of extracellular components in the reactor such as substrates, products and biomass, $\mathbf{S_x}$ is the $(n_x \times n_r)$ stoichiometric matrix, and $\mathbf{Z}$ is the $(n_r \times n_z)$ EM matrix, $\mathbf{r_M}$ is the vector of n_z fluxes through EMs, and D is dilution rate. By setting $D = 0$, Eq. 1 also represents a batch reactor model. Fluxes through EMs are given as below:

$$r_{M,j} = v_{M,j}\left(e_{M,j}/e_{M,j}^{\max}\right) r_{M,j}^{\mathrm{kin}} \tag{2}$$

where the subscript j denotes the index of EM, $v_{M,j}$ is the cybernetic variable controlling enzyme activity, $e_{M,j}$ and $e_{M,j}^{\max}$ are the enzyme level and its maximum value, respectively, and $r_{M,j}^{\mathrm{kin}}$ is the kinetic term. Enzyme level $e_{M,j}$ is obtained from the following dynamic equation, i.e.,

$$\frac{de_{M,j}}{dt} = \alpha_{M,j} + u_{M,j} r_{ME,j}^{\mathrm{kin}} - \beta_{M,j} e_{M,j} - \mu e_{M,j} \tag{3}$$

where the first and second terms of the right-hand side denote constitutive and inducible rates of enzyme synthesis, and the last two terms represent the decrease of enzyme levels by degradation and dilution, respectively. In the second term of the right-hand side, $u_{M,j}$ is the cybernetic variable regulating the induction of enzyme synthesis, and $r_{ME,j}^{\mathrm{kin}}$ is the kinetic part of inducible enzyme synthesis rate. In the third and fourth terms, $\beta_{M,j}$ and μ are the degradation and specific growth rates, respectively. μ is given as an element of $\mathbf{S_x Z r_M}$ corresponding to biomass in Eq. 1. The cybernetic control variables, $u_{M,j}$ and $v_{M,j}$ are computed from the Matching and Proportional laws,[7,8] respectively:

$$u_{M,j} = \frac{p_j}{\sum_k p_k}; \quad v_{M,j} = \frac{p_j}{\max_k(p_k)} \tag{4}$$

where the return-on-investment p_j denotes the carbon uptake flux through the jth EM.

HCM for anaerobic E. coli *growth*

The foregoing formulation applies to modeling anaerobic growth of *E. coli* GJT001 on glucose and pyruvate. Model is developed along the following procedures: (i) construction of metabolic network, (ii) network decomposition into EMs and their reduction, and (iii) parameter identification. The metabolic network is constructed by expanding the network used in Young et al. (2008)[9] to include assimilation of pyruvate and reversed glycolysis reactions. The resulting network contains 14 reactions (1 reversible and 13 irreversible), and 18 metabolites (8 extracellular and 10 intracellular) (Figure 1; Supporting Information Tables 1 and 2). The network is decomposed into 49 EMs using METATOOL 5.1.[10] Model simplification, enabled by using the minimum number of modes to represent yield data of fermentation products,[11] leads to extraction of four core modes (Supporting Information Table 3). The yield data suggest that four EMs provided sufficient pathway options for the organism to respond to conditions used in our experiments. Kinetic equations are given as follows:

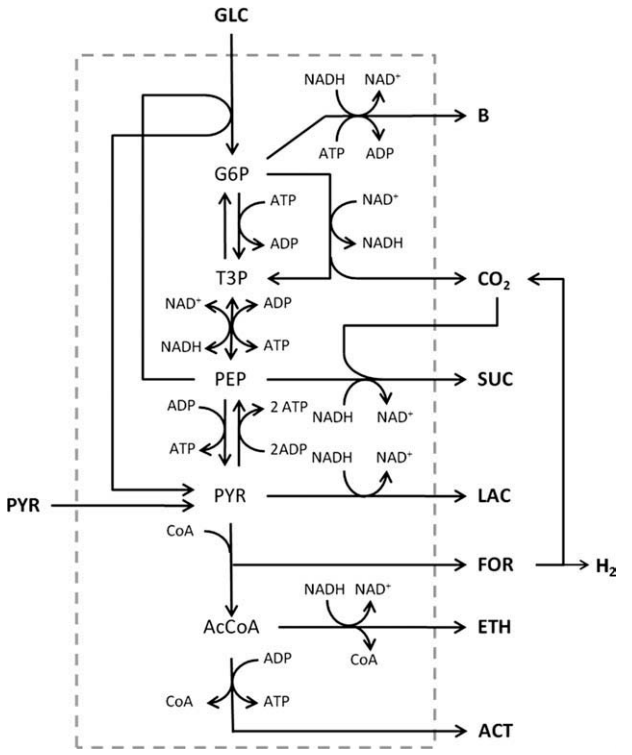

Figure 1. Metabolic network of anaerobic *E. coli* growth on glucose and pyruvate. Letters outside and inside the dashed gray box denotes extracellular and intracellular metabolites, respectively. The full names of metabolites are provided in Supporting Information Table 1.

$$r_{M,j}^{\mathrm{kin}} = \begin{cases} k_1^{\max} \frac{x_G}{K_{G,1}+x_G} & (j=1) \\ k_2^{\max} \frac{x_P}{K_{P,2}+x_P} & (j=2) \\ k_j^{\max} \frac{x_G}{K_{G,j}+x_G} \frac{x_P}{K_{P,j}+x_P} & (j=3,4) \end{cases} \tag{5}$$

$$r_{ME,j}^{\mathrm{kin}} = \begin{cases} k_{E,1} \frac{x_G}{K_{G,1}+x_G} & (j=1) \\ k_{E,2} \frac{x_P}{K_{P,2}+x_P} & (j=2) \\ k_{E,j} \frac{x_G}{K_{G,j}+x_G} \frac{x_P}{K_{P,j}+x_P} & (j=3,4), \end{cases}$$

where the subscripts G and P denote glucose and pyruvate.

The decomposition of formate into hydrogen and carbon dioxide is also considered in the model. Then, for formate, Eq. 1 is modified by including an additional term $-r_F c$ in the right hand side. The kinetic form of r_F is given as follows[9]:

Table 1. Optimized Parameter Values of the HCM for Anaerobic Growth of *E. coli*

j	k_j^{max} (mmol/gDW/h)	$K_{G,j}$ (mM)	$K_{P,j}$ (mM)	$\alpha_{M,j}$ (h^{-1}) (fixed)	$\beta_{M,j}$ (h^{-1}) (fixed)	$k_{E,j}$ (h^{-1})*
1	0.394 ± 0.013	0.08 ± 0.42	–	0.004	0.05	0.44
2	0.171 ± 0.005	–	0.07 ± 0.19	0.004	0.05	0.217
3	0.410 ± 0.016	0.133 ± 0.78	0.8 ± 1.63	0.004	0.05	0.456
4	0.339 ± 0.013	0.04 ± 0.22	0.2 ± 0.87	0.004	0.05	0.385

The subscript j denotes the index for EMs ($*k_{E,j}$ is set to be $k_j^{max} + \beta_{M,j} - \alpha_{M,j}$ so that maximum enzyme levels become unity).

$$r_F = k_F \frac{x_F^2}{K_F^2 + x_F^2} \tag{6}$$

where the subscript F denotes formate.

MATLAB 7.1 (Mathworks, Natick, MA) is used for dynamic simulations and parameter optimization. Transient simulation curves are generated by solving ordinary differential equations given in Eqs. 1 and 3 using ode15s.m. Optimal values of parameters including maximum reaction rate constants (k_j^{max}'s), and Michaelis constants ($K_{G,j}$'s, and $K_{P,j}$'s) are identified using the nonlinear optimization function lsqnonlin.m such that the sum of squared errors between model simulations and batch data are minimized. Optimal values for k_F and K_F are taken from Kim et al. (2008)[1] as 7.998 and 6.997, respectively, and all other parameters are presented together with their confidence intervals in Table 1. The Michaelis constants were initially set at available past estimates and subsequently corrected by optimization along with all the rate constants. Michaelis constants varied only slightly from their initial guesses reflecting their limited sensitivity. More details on numerical simulation and parameter identification are referred to Kim (2008).[12]

Experiments

Strain

A significant genotype of *E. coli* strain GJT001 (spontaneous cadR mutant of MC4100, (ATC35695) Δlac(arg-lac)U169 rpsL150 relA1 ptsF, SmR)[13] was used in this study. GJT001 anaerobic shows wild-type glucose metabolism and can grow in anaerobic conditions.

Culture Medium. (a) M9 minimal medium: The medium is composed of Na_2HPO_4 (30 g/L), KH_2PO_4 (15 g/L), NH_4Cl (5 g/L), and NaCl (2.5 g/L), and modified SL-7 trace element solution. (b) Modified SL-7 trace element solution: HCl (6.5 mL/L), $MgSO_4$(120mg/L), $CaCl_2$(11.1 mg/L), $FeSO_4.7H_2O$ (2.1 mg/L), H_3BO_3 (60 mg/L), $MnCl_2.4H_2O$ (100 mg/L), $CoCl_2.6H_2O$ (120 mg/L), $ZnSO_4.7H_2O$ (145 mg/L), $NiCl_2.6H_2O$ (25 mg/L), $CuSO_4.5H_2O$ (25 mg/L), $Na_2MoO_4.2H_2O$ (25 mg/L), Na_2SeO_3 (20 mg/L).

Batch Experiments

• Medium: M9 minimal medium was used. The concentration of glucose and pyruvate were adjusted accordingly for parameter identification. For anaerobic flask cultures, the medium was 100 mM MOPS (3-(*N*-morpholino) propanesulfonic acid) buffer to stabilize pH and 10 mM $NaHCO_3$ to reduce the initial lag times.

• Cultivation: Preculturing was carried out aerobically in overnight shake flasks. Before inoculation, 60 mL of fresh medium was sparged with sterile nitrogen gas to establish anaerobic conditions. The culture was then inoculated to an initial OD 600 of ~0.2. Anaerobic shake flask cultures were grown in sealed 100 mL serum vials at 37°C with rotary shaking at 100 rpm. Samples were periodically withdrawn through a septum using a syringe and needle to avoid oxygen contamination.

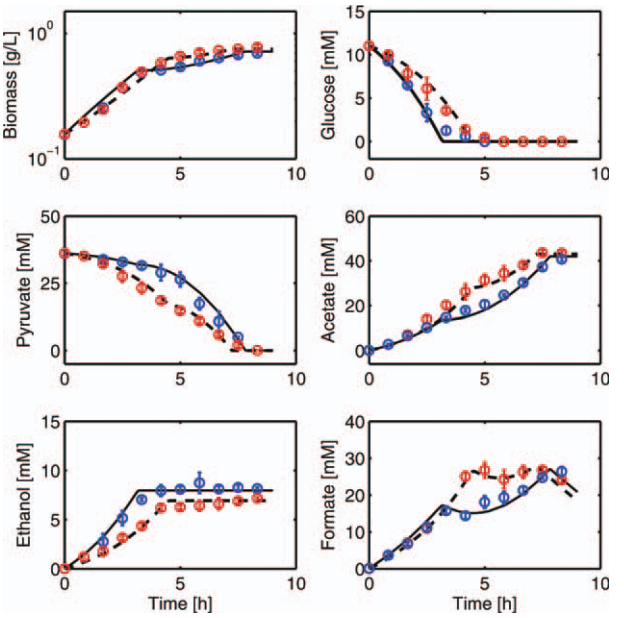

Figure 2. Batch experiments for anaerobic *E. coli* growth on glucose-pyruvate mixtures. Blue and red symbols denote experimental data when cells are precultured on glucose and pyruvate, respectively, and solid and dashed lines indicate simulation curves using the HCM. Simultaneous uptake patterns were observed with cells precultured on pyruvate, while sequential or diauxic growth occurred with cells precultured on glucose. The model fits both patterns well. The model shows simultaneous pattern for cells precultured on pyruvate as initial enzyme levels for pyruvate metabolism were high enough to favor EMs for simultaneous utilization of pyruvate and glucose. Preculturing on glucose, in contrast, favors selection of modes taking up glucose. Both preferences above, made in the interest of maximizing carbon uptake rate, are enabled through the cybernetic variables.

Chemostat Experiments

• Medium: M9 minimal medium at pH 7.0 was used in all experiments. 10 mM $NaHCO_3$ was added to reduce initial lag time. Also, antifoam of 6 μL/L was added to prevent the culture from forming foam. All chemicals used in the experiments were reagent grade and obtained from Aldrich or other international suppliers.

• Cultivation (I): Continuous culture experiments, reported in Figures 3 and 4, were carried out in a 3 L Biostat B plus (Sartorius Stedim, Germany) stirred and jacketed glass bioreactor, equipped with OD (optical density), DO (dissolved oxygen), pH and temperature probes and connected to peristaltic pumps for flow rate, pH/antifoam control. Nitrogen was continuously sparged at a flow rate of 0.5 L/min and the culture broth (working volume of 1.5 L) maintained at a temperature of 37°C, was agitated at 100 rpm using a standard disk turbine. A condenser maintained at 2–4°C was attached at the vent line of the fermenter to prevent loss of fermentation products. The bioreactor pH was controlled at pH 7 by controlling additions of 2N NaOH and 2N HCl solutions. The input flow rate was controlled using a BioRad Econo pump with a 1.6 mm tube (0.6 mm ID) so that the

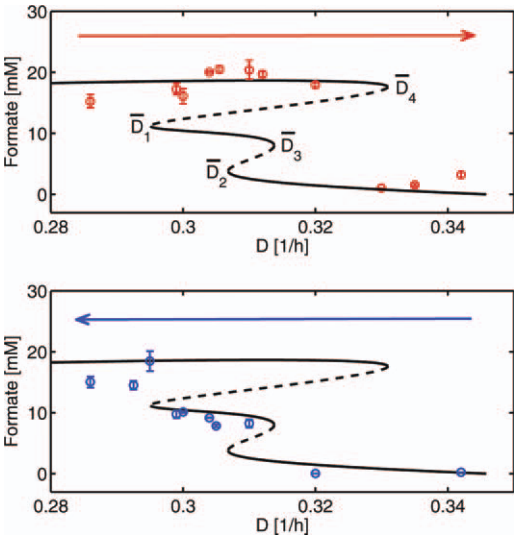

Figure 3. Steady state concentrations of formate in a chemostat with 10 mM glucose and 15 mM pyruvate feed (40 mol % glucose). Symbols and lines denote experimental data and model prediction, respectively. Error bars denote standard deviations of data. Solid and dashed lines indicate stable and unstable states predicted by the HCM. At the top, experimental data (red symbols) are collected along the increasing direction of dilution rate D. At the bottom, experimental data (blue symbols) are collected along the decreasing direction of dilution rate D. Raw data are provided in a separate file.

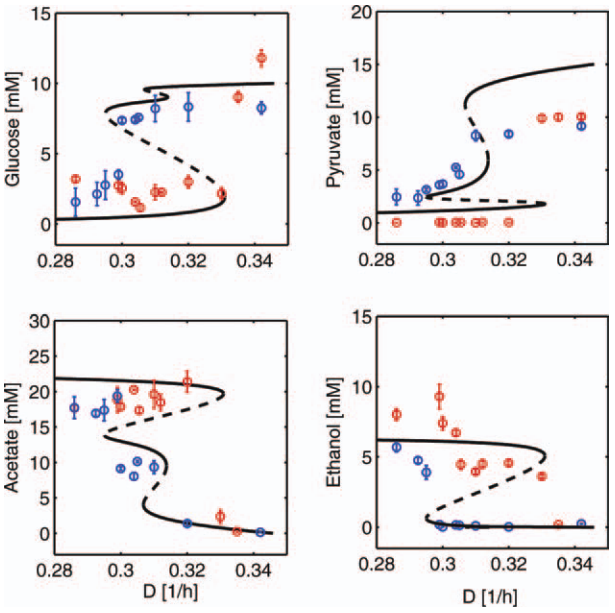

Figure 4. Multiple steady states for 10 mM glucose and 15 mM pyruvate feed (40 mol % glucose). Red and blue symbols represent experimental extracellular measurements collected along the increasing and decreasing direction of dilution rate D. Solid and dashed lines denote stable and unstable states predicted by the model.

flow rates could be controlled in the range of 0.01–5 mL/min with an accuracy of ±5%. The output flow from the reactor was also controlled by another peristaltic pump which was regulated by the level controller. Level control was necessitated since the bioreactor pH was maintained at 7 by

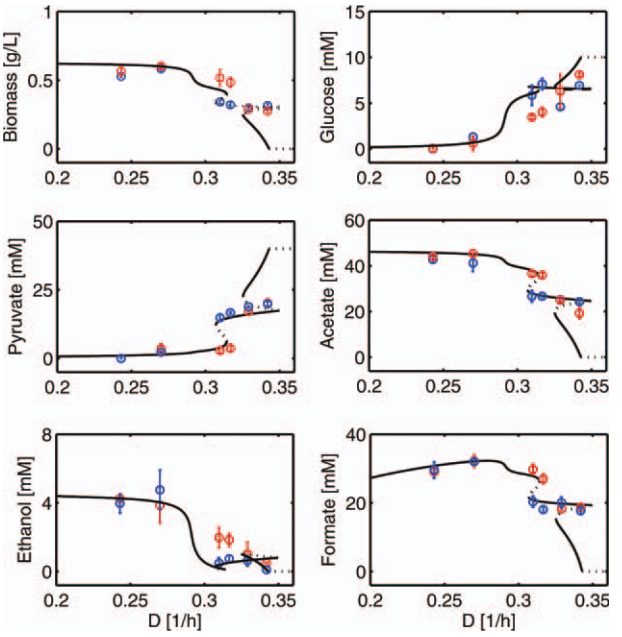

Figure 5. Multiple steady states for 10 mM glucose and 40 mM pyruvate feed (20 mol % glucose). Red and blue symbols represent experimental extracellular measurements collected along the increasing and decreasing direction of dilution rate D. Solid and dotted lines denote stable and unstable states predicted by the model.

controlling additions of 2N NaOH and 2N HCl solutions through system pumps. Since the additions were less than 1 mL at any time and in intervals of more than 15 min, the changes in flow rate and levels were not significant. The turbidity (as OD) of the culture broth was continuously measured using the Fundalux II (Sartorius Stedium) on-line turbidity measurement probe. The dissolved oxygen level in the culture broth was continuously monitored using the DO probe. M9 minimal medium containing 5 g/L glucose was used as the initial fermentation medium which was inoculated to an initial OD of about 0.1. The mode of operation was shifted from batch to chemostat at the end of the exponential growth phase, which was typically characterized by an OD of about 0.5. Continuous feed to the chemostat consisted of the M9 minimal medium containing $NaHCO_3$ and modified SL-7 trace element solution, with 10 mM glucose and 15 mM sodium pyruvate. Dilution rates were varied in the range of 0.286–0.342 h^{-1} through the Biorad pump and the multiple number of experiments involved stepwise increase in dilution rates followed by a stepwise decrease. During continuous culture, the steady state was assumed to have been attained by satisfying two conditions: (1) the running time of bioreactor at one specific dilution rate was at least equal to or larger than five times the residence time and (2) the OD is constant for 4 hours.

- Cultivation (II): Continuous culture experiments reported in Figure 5 were carried out in a 3.7 L (working volume of 2.0 L) BioFloIII (New Brunswick), stirred at 150 rpm, where nitrogen was sparged at a flow rate of ~0.8 L/min. The bioreactor pH was controlled at pH 7.0 by controlling additions of 8 M NaOH and 2N HNO_3 solutions.. Continuous feed to the chemostat was the M9 minimal medium containing antifoam, $NaHCO_3$, 10 mM glucose and 40 mM pyruvate. Dilution rates were varied in the range of 0.243–0.342 h^{-1}. All

other conditions are maintained to be the same as in Cultivation (I).

Analytical Techniques

• Cell density was monitored at 600 nm in a spectrophotometer.

• The samples were centrifuged at 10,000 rpm for 7–10 min, washed with 0.15 M sodium chloride solution, and dried in an oven until a constant weight was obtained. The normal duration of drying was ~18 hours. The conversion factor from OD to cell density was ~0.471 g-biomass/OD. For fermentation products, broth samples were collected and centrifuged at 10,000 rpm for 7–10 min. The supernatant was stored in −20°C refrigerator for later HPLC analysis.

• Fermentation products were identified using Agilent HPLC system equipped with an Aminex HPX-87H cation exchange column(s) (Biorad Laboratories, MO). A mobile phase of 10 mM sulfuric acid was used at a flow rate of 0.6 mL/min for metabolites studied in Figure 3 and 4 while 5 mM sulfuric acid was used at a flow rate of 0.8 mL/min for metabolites studied in Figure 5. The temperature along the column was maintained at 65°C. The level of pyruvate, succinate, lactate, acetate and formate in culture medium was analyzed with a UV detector at a wavelength of 210 nm; while the concentration of glucose and ethanol was analyzed by Refractive Index (RI) detector. When there is significant RI response overlap between glucose and pyruvate, the samples were diluted 10 times to alleviate any signal interference.

Results and Discussion

Model identification from batch growth data

HCM has been successfully used to model *E. coli* growth on mixed carbon source (glucose and pyruvate) by Kim et al. (2008).[1] In this model, different uptake patterns of glucose and pyruvate can be experimentally validated depending on whether the bacteria were initially cultivated on glucose or on pyruvate. Different uptake patterns of glucose and pyruvate found experimentally depending on whether the bacteria were previously cultured on glucose or on pyruvate could be predicted by the model (Figure 2). While this would appear to lend support to the cybernetic concept of maximizing carbon uptake rate, we describe below a more exacting scenario for experimental evidence of the same.

Description of a continuous fermentation system

We consider a chemostat in which the bacteria are continuously fed with a mixture of glucose and pyruvate at a constant rate with simultaneous withdrawal of the well-stirred culture at an equal rate. The issue of interest is the attainment of steady state within the chemostat when cells wash out at the same rate at which they multiply. Steady state must of course be preceded by a transient period starting from some initial instant. As the medium flows into the chemostat, the cells respond by manipulating pathway options (as dictated by the model) to consume glucose and pyruvate in proportions that will maximize the carbon uptake rate at each instant of time. The maximization of carbon flux into the cell is of course subjected to the uptake kinetics of the 4 EMs identified from experimental data. Under these circumstances, any given pathway option could be used to varying extents (or at the extreme even eliminated from use). The cells will continue adapting to the new environment through a transient period until a steady state is achieved when the optimal operation of pathway becomes time-independent. As a result, system variables such as biomass, substrate and products will also reach steady state. Young and Ramkrishna (2007)[8] have demonstrated in considerable detail how the pathway options selected by cybernetic models are indeed optimal.

Hysteresis behavior predicted by the model

Of particular interest to the chemostat scenario is the possibility, revealed through calculations, that the steady state reached by the organism could depend on its initial state. Such a calculation was enabled by first identifying model parameters from dynamic experimental concentration data on substrates, biomass, and various fermentation products. The model parameters were fitted only to batch growth data obtained with glucose and pyruvate carbon sources. In other words, no chemostat data were involved in parameter determination. Subsequent numerical computation from the nonlinear ordinary differential equations revealed that the metabolic states in the chemostat at steady state are not unique under certain circumstances. The conditions were characterized by the dilution rate D and the fraction of glucose in the substrate mixture γ in the feed to the chemostat. Figure 3 shows the steady state concentration of formate, one of the fermentation products, as a function of the dilution rate for a particular value of $\gamma(= 0.4)$. Within this window, the steady state reached for a particular dilution rate, say D_1, starting from a steady state at another dilution rate D_2, for reasons to follow, may depend upon whether $D_1 > D_2$ or $D_1 < D_2$. It is obvious that without the guidance of model simulation providing the narrow region of multiplicity, an experimental effort towards determining it would involve exhaustively covering the entire range of dilution rates.

True source for hysteresis

The *hysteresis* phenomenon encountered above is of course familiar aspect of nonlinear behavior of chemical reaction systems.[14] It is important to note here that the hysteresis is a product of the nonlinearity as well as the metabolic shift that the cybernetic variables initiate. This implication of the role of cybernetic regulation in the observed multiplicity, can be recognized as follows. If the cybernetic variables u_i, v_i are set to one (i.e., eliminating regulatory effects), even the model fit of the dynamic data is seriously compromised; thus the model cannot be used to address multiplicity. Multiple steady states are attained (Supporting Information Figure 1), when multiple sets of reactions are available at the same dilution rate for activation towards achieving the metabolic objective.

Experimental verification

Consider the "turning points" in Figure 3, identified as $\bar{D}_1, \bar{D}_2, \bar{D}_3$ and $\bar{D}_4$ in increasing order. If we pick D_1 and D_2 to be both less than $\bar{D}_1$, the steady state attained would not depend on whether $D_2 < D_1$ or $D_2 > D_1$. A similar thing can be said of picking D_1 and D_2 to be both greater than $\bar{D}_4$. Suppose, however, that we increase the dilution rate from less than $\bar{D}_1$; the steady states predicted for formate would vary along the top branch until reaching $\bar{D}_4$. Along this

branch the implication is that the organism is adhering to pathway options changing only in small quantitative measures whereas with a very small increase in dilution rate beyond $\bar{D}_4$, the formate production drops precipitously! Of course this drop is not to be viewed as "sudden" in a temporal sense as we are dealing with steady state behavior; nevertheless, on changing from a dilution rate D_2 just left to $\bar{D}_4$ to a dilution rate $D_1 > \bar{D}_4$, the organism is predicted to make a quick switch of its pathway options towards maximizing the carbon uptake rate resulting in a significantly lower formate production. What is true of formate is also true of other fermentation products such as acetate, ethanol and so on (Figure 4). Next consider experiments at dilution rates decreasing from above $\bar{D}_4$. The organism is predicted to continue along the lower branch of steady states with gradually increasing fermentation levels until after reaching $\bar{D}_2$ when again a switch occurs to a higher fermentation level along an intermediate branch. Further decrease of the dilution rate results again in gradually increasing fermentation levels until at $\bar{D}_1$ there is again a step change in pathway option with a spurt in fermentation activity. The predicted phenomena should now be evident from further inspection of Figure 3. It should also be clear that they provide the challenging scenario we sought to put the cybernetic goal of maximizing the uptake rate of carbon to a rigorous test.

Hysteresis arises also for other values of γ with varying multiplicity (Figure 5). Thus for $\gamma = 0.2$, two stable steady states are predicted that are confirmed by experiments as well.

Raw data for Figures 3–5 are provided as Supporting Information (see data file).

Animated results

For effective communication of our experimental effort we provide a video clip containing the theoretical predictions in Figure 3 (see Supporting Information). The data are introduced first as an animated sequence from a low dilution rate ($<\bar{D}_1$) increasing to above $\bar{D}_4$, and second from a high dilution rate ($> \bar{D}_4$) decreasing past $\bar{D}_1$. The foregoing exercise will indeed show that the data are in conformity with prediction for formate as well as the other fermentation products, cell mass and the substrates. In drawing this inference, concession must be made for proximity of the data to prediction because of different measurement errors as well as drastic model approximations due to reducing pathway options.

Conclusions

Although cybernetic models have been validated in the past by successful prediction of various uptake patterns of mixed carbon substrates,[1,7,15] this article shows that metabolic multiplicity behavior, implied by the cybernetic nonlinearity, is remarkably reproduced by experiments. This behavior is a consequence of shifting emphasis of the organism on the use of pathway options rather than that of nonlinearity of the kinetics. However, as per the cited work of Lei et al. (2001),[2] a kinetic model suitably expanded to account for regulatory effects can also reproduce such multiplicity of metabolic states.

Because the cybernetic model has the potential to describe metabolic regulation at large, it is likely that the multiplicity can extend considerably to include numerous subtly different metabolic states. The demonstration of metabolic multiplicity has been limited to extracellular variables in this article, it indeed raises the question of how intracellular fluxes, gene expression profiles, and numerous other measures of metabolic behavior would serve to provide additional corroboration of such cybernetic predictions. An effort in this direction is already in progress at Purdue's Center for Science of Information funded by the National Science Foundation.

Acknowledgment

The authors gratefully acknowledge a special grant from Dean's Research Office, Purdue University. A Senior Research Fellowship for Sunil R. Sunkara and the fermentation facility at the DBT-ICT Centre for Energy Biosciences both funded by the Department of Biotechnology, Ministry of Science & Technology of the Government of India. Partial support by the Center for Science of Information (CSoI), an NSF Science and Technology Center, under grant agreement CCF-0939370.

Notation

Symbols

c = biomass concentration, g/L
D = dilution rate, 1/h
$e_{M,j}$ = level of enzyme which catalyzes the flux through the jth elementary mode
$e_{M,j}^{\max}$ = maximal level of $e_{M,j}$
k_F = rate constant for formate decomposition
$k_j^{\max}$ = maximal rate constant for the flux through the jth elementary mode, mmol/(gDW h)
K_F = Michaelis constant for the flux through the jth elementary mode, mM
$K_{G,j}$ = Michaelis constant for the flux through the jth elementary mode, mM
$K_{P,j}$ = Michaelis constant for the flux through the jth elementary mode, mM
p_j = return-on-investment
r_F = specific rate of formate decomposition into CO_2 and H_2, mmol/(gDW h)
$r_{M,j}$ = flux through the jth elementary mode, mmol/(gDW h)
$r_{M,j}^{\text{kin}}$ = unregulated flux through the jth elementary mode (i.e., kinetic part in $v_{M,j}$), mmol/(gDW h)
$r_{ME,j}^{\text{kin}}$ = kinetic part of inducible enzyme synthesis rate, 1/h
$\mathbf{r_M}$ = flux vector through elementary modes, mmol/(gDW h)
$\mathbf{S_x}$ = stoichiometric matrix
t = time, h
$u_{M,j}$ = cybernetic variable regulating the induction of enzyme which catalyzes the flux through the j the elementary mode
$v_{M,j}$ = cybernetic variable regulating the activity of enzyme which catalyzes the flux
x_G = concentration of glucose, mM
x_P = concentration of pyruvate, mM
$\mathbf{x}$ = concentration vector of extracellular metabolites including substrates, mM; products, mM; and biomass, g/L
$\mathbf{x_{IN}}$ = concentration vector of extracellular metabolites in the feed, mM
$\mathbf{Z}$ = matrix with elementary modes as column vectors through the j the elementary mode

Greek letters

$\alpha_{M,j}$ = constitutive enzyme synthesis rate, 1/h
$\beta_{M,j}$ = rate of enzyme degradation, 1/h
γ = mole fraction of glucose in the substrate mixture in the feed to the chemostat
μ = specific growth rates, 1/h

Acronyms

EM = elementary mode
HCM = hybrid cybernetic model
OD = optical density

Literature Cited

1. Kim JI, Varner JD, Ramkrishna D. A hybrid model of anaerobic *E. coli* GJT001: combination of elementary flux modes and cybernetic variables. *Biotechnol Prog*. 2008;24:993–1006.
2. Lei F, Rotboll M, Jorgensen SB. A biochemically structured model for Saccharomyces cerevisiae. *J Biotechnol*. 2001;88: 205–221.
3. Song HS, Morgan JA, Ramkrishna D. Systematic development of hybrid cybernetic models: application to recombinant yeast co-consuming glucose and xylose. *Biotechnol Bioeng*. 2009;103: 984–1002.
4. Ramkrishna D. A cybernetic perspective of microbial-growth. *ACS Symp Ser*. 1983;207:161–178.
5. Ramkrishna D, Kompala DS, Tsao GT. Are microbes optimal strategists. *Biotechnol Progr*. 1987;3:121–126.
6. Schuster S, Fell DA, Dandekar T. A general definition of metabolic pathways useful for systematic organization and analysis of complex metabolic networks. *Nat Biotechnol*. 2000;18:326–332.
7. Kompala DS, Ramkrishna D, Jansen NB, Tsao GT. Investigation of bacterial-growth on mixed substrates - experimental evaluation of cybernetic models. *Biotechnol Bioeng*. 1986;28: 1044–1055.
8. Young JD, Ramkrishna D. On the matching and proportional laws of cybernetic models. *Biotechnol Progr*. 2007;23:83–99.
9. Young JD, Henne KL, Morgan JA, Konopka AE, Ramkrishna D. Integrating cybernetic modeling with pathway analysis provides a dynamic, systems-level description of metabolic control. *Biotechnol Bioeng*. 2008;100:542–559.
10. von Kamp A, Schuster S. Metatool 5.0: fast and flexible elementary modes analysis. *Bioinformatics*. 2006;22:1930–1931.
11. Song HS, Ramkrishna D. Reduction of a set of elementary modes using yield analysis. *Biotechnol Bioeng*. 2009;102:554–568.
12. Kim JI. A hybrid cybernetic modeling for the growth of *Escherichia coli* in glucose-pyruvate mixtures. Ph.D. Thesis, Purdue University, West Lafayette, IN, 2008.
13. Tolentino GJ, Meng SY, Bennett GN, San KY. A pH-regulated promoter for the expression of recombinant proteins in *Escherichia coli*. *Biotechnol Lett*. 1992;14:157–162.
14. Vejtasa SA, Schmitz RA. An experimental study of steady state multiplicity and stability in an adiabatic stirred reactor. *AIChE J*. 1970;16:410.
15. Ramakrishna R, Ramkrishna D, Konopka AE. Cybernetic modeling of growth in mixed, substitutable substrate environments: preferential and simultaneous utilization. *Biotechnol Bioeng*. 1996;52:141–151.

Manuscript received Apr. 19, 2012, and revision received Jun. 1, 2012.